Supplementary Material: Ice nucleating particles over the Eastern Mediterranean measured by unmanned aircraft systems

Jann Schrod[1], Daniel Weber[1], Jaqueline Drücke[1], Christos Keleshis[2], Michael Pikridas[2], Martin Ebert[3], Bojan Cvetković[4], Slobodan Nickovic[4], Eleni Marinou[5,6], Holger Baars[7], Albert Ansmann[7], Mihalis Vrekoussis[2,8,9], Nikos Mihalopoulos[2,10], Jean Sciare[2], Joachim Curtius[1], and Heinz G. Bingemer[1]

[1]Institute for Atmospheric and Environmental Sciences, Goethe University Frankfurt, 60438 Frankfurt am Main, Germany
[2]Energy, Environment and Water Research Center, The Cyprus Institute, Nicosia, 2121 Aglantzia, Cyprus
[3]Institute for Applied Geosciences, Technical University of Darmstadt, 64287 Darmstadt, Germany
[4]Republic Hydrometeorological Service of Serbia, 11000 Belgrade, Serbia
[5]Institute for Astronomy, Astrophysics, Space Applications and Remote Sensing, National Observatory of Athens, 15236 Athens, Greece
[6]Department of Physics, Aristotle University of Thessaloniki, 54124 Thessaloniki, Greece
[7]Leibniz Institute for Tropospheric Research, 04318 Leipzig, Germany
[8]Institute of Environmental Physics and Remote Sensing - IUP, University of Bremen, 28359 Bremen, Germany
[9]Center of Marine Environmental Sciences - MARUM, University of Bremen, 28359 Bremen, Germany
[10]Institute for Environmental Research and Sustainable Development, National Observatory of Athens, 15236 Athens, Greece

Correspondence to: Jann Schrod (schrod@iau.uni-frankfurt.de)

Supplementary Material

1 Aethalometer measurements during INP sampling

In order to identify any potential contamination, aerosol absorption was simultaneously monitored using a micro aethalometer (AethLabs, Model AE51) during each flight with Cruiser. The aethalomter's inlet was approximately 7 cm away from that of the INP sampler, ensuring that both instruments sampled the same air masses. Measurements from the aethalometer during each sampling are provided in Fig. S1. Although considerably noisy, these data do not show any significant large spikes that indicate particulate contamination.

2 Estimate of errors from anisokinetic sampling

The diameter D_s of the sample inlet nozzle was such that near isokinetic sampling (i.e. the air sample inlet velocity U equals the air speed U_0 of the UAS) was achieved for the average operational air speed U_0 of the UAS and the mean aerosol sampling rate Q. The three quantities U_0, D_s and Q are related by Eq. 1:

$$D_\mathrm{s} = 2\sqrt{\frac{Q}{\pi U_0}}, \tag{1}$$

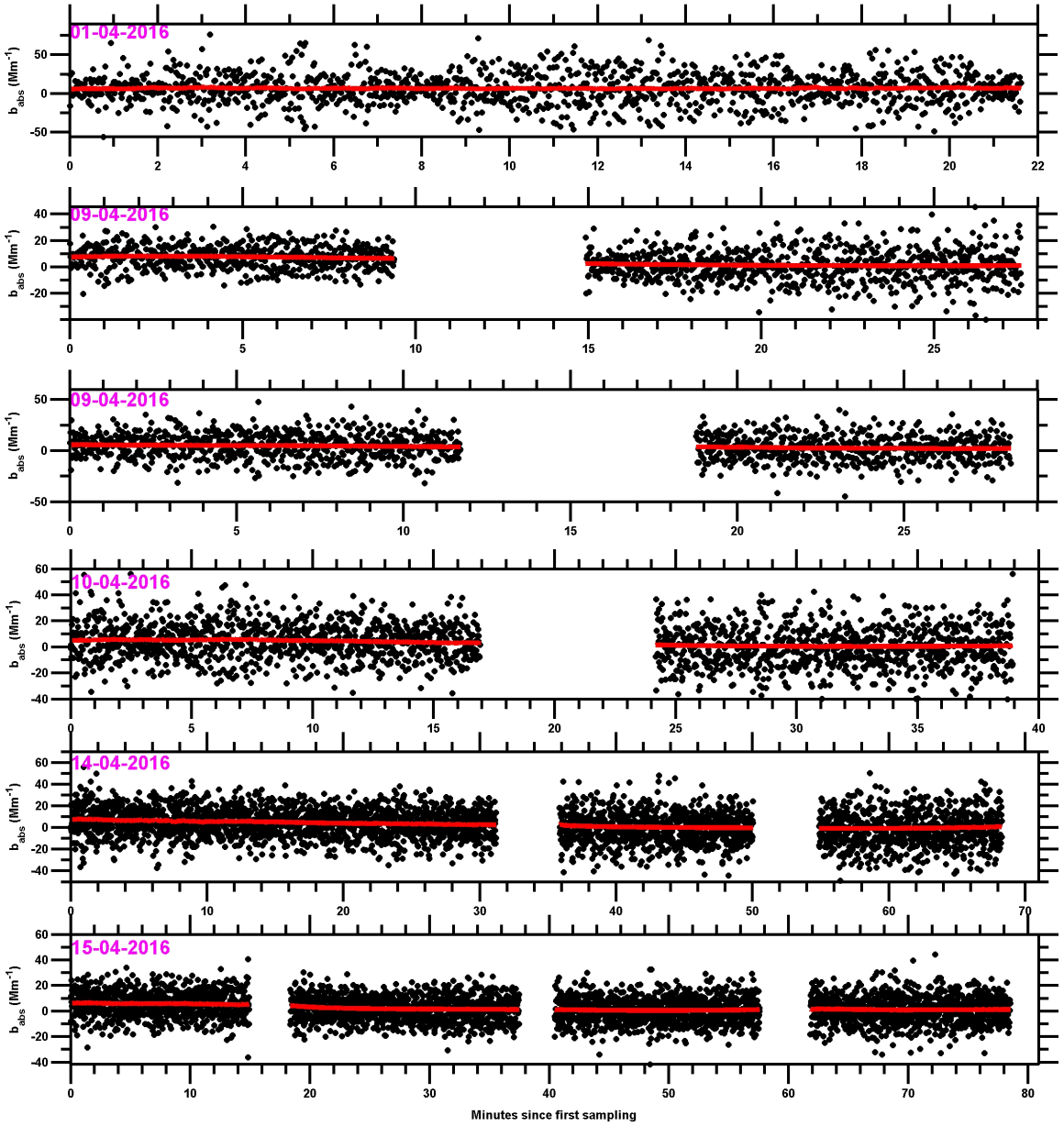

Figure 1. Ambient aerosol absorption during INP sampling onboard the Cruiser. The raw output (black dots) and a rolling average (red line, based on a modification method of Hagler et al. (2011)) are shown. No indication of contamination by the two stroke engine's exhaust was identified.

For the mean operational conditions these parameters are: a) for Cruiser: $U_0 = 27.8\,\mathrm{ms}^{-1}$, $Q = 5\,\mathrm{lpm}$, $D_s = 1.95\,\mathrm{mm}$; and b) for Skywalker: $U_0 = 16.7\,\mathrm{ms}^{-1}$, $Q = 5\,\mathrm{lpm}$, $D_s = 2.52\,\mathrm{mm}$.

In the following we estimate sampling errors due to anisokinetic conditions (i.e. $U \neq U_0$). The latter may arise when the UAS spirals in the wind field and air speed U_0 and pump rate Q deviate from conditions a) or b) due to tail wind or head wind. The range of U_0 and Q observed during the campaign is given in Tab. S1. All parameters vary typically by less than 20%. Our estimate follows the discussion of sampling errors in Hinds (1999), chapter 10. For simplicity's sake and for the lack of other measurements, we will use the assumption that the gas streamlines entering the sampling inlet show no misalignment whatsoever. For this idealized case the ratio of the aerosol number concentration C at $U \neq U_0$ to C_0 at isokinetic conditions is then given by Belyaev & Levin (1974):

$$\frac{C}{C_0} = 1 + \left(\frac{U_0}{U} - 1\right)\left(1 - \frac{1}{1 + \left(2 + 0.62\frac{U}{U_0}\right) Stk}\right), \tag{2}$$

with the Stokes number Stk being defined by

$$Stk = \frac{\tau U_0}{D_s}, \tag{3}$$

and the relaxation time τ being

$$\tau = \frac{\rho_p d^2 C_C}{18\eta}. \tag{4}$$

Here ρ_p is the particle density (estimated for dust as $2.6\,\mathrm{g\,cm^{-3}}$), d is the aerosol diameter, C_c is the Cunningham correction factor and η is the viscosity of the air.

Table 1. Variation of sample flow Q and airspeed U_0 during the campaign.

	Skywalker	Cruiser
Q_{mean} [lpm]	4.91	
Q_{min} [lpm]	4.37	
Q_{meax} [lpm]	5.56	
$U_{0,\,\mathrm{mean}}$ [m/s]	17.4	28.1
$U_{0,\,\mathrm{min}}$ [m/s]	14.3	23.4
$U_{0,\,\mathrm{meax}}$ [m/s]	23.5	33.3

Figures S2 and S3 present C/C_0 as calculated by Eq. 2 as function of particle size for the mean, maximum and minimum Q and U_0 occurring during flights of Cruiser and Skywalker at an altitude of 2000 m. The maximum error is negligible for particles below 1 µm, and grows with increasing particle size up to around ± 30% for particles of 10 µm in diameter for Cruiser and up to ± 60% for Skywalker.

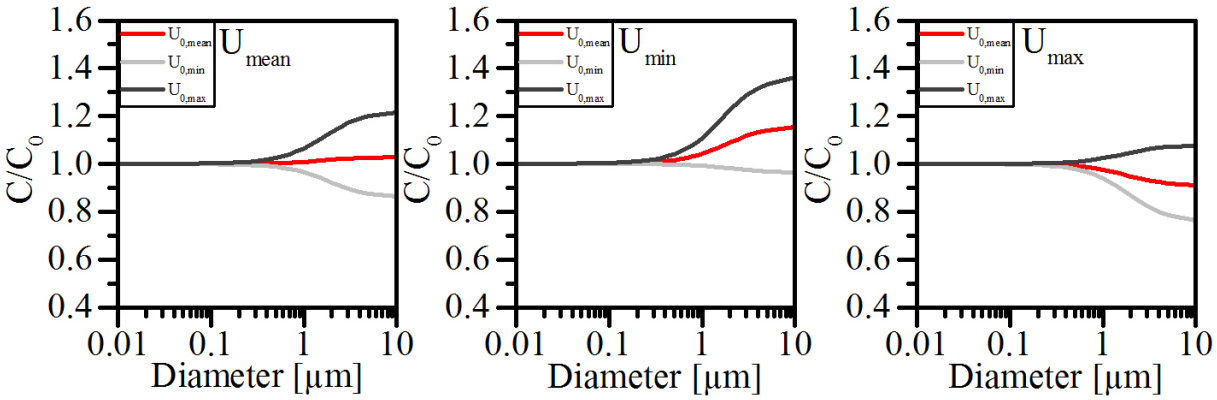

Figure 2. Aerosol number concentration ratio due to anisokinetic sampling effects as a function of particle diameter for Cruiser.

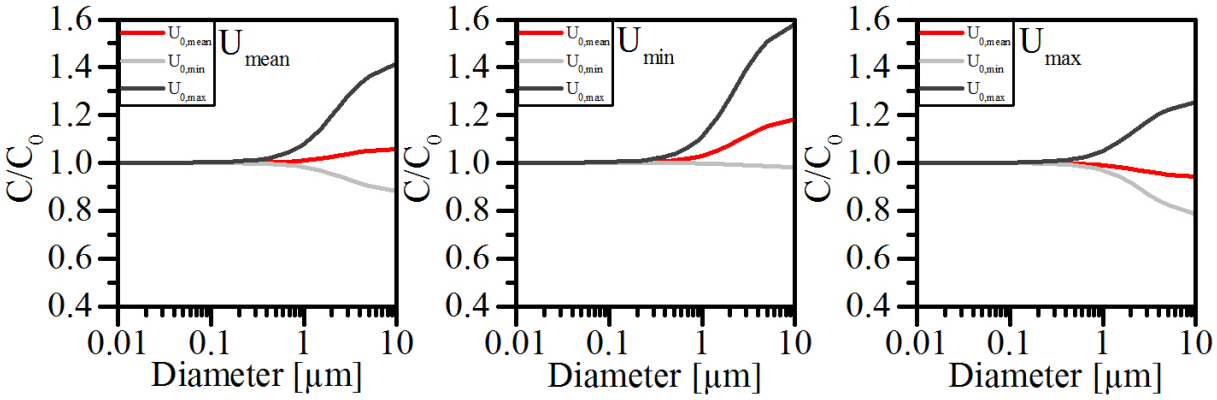

Figure 3. Aerosol number concentration ratio due to anisokinetic sampling effects as a function of particle diameter for Skywalker.

3 Results of the DREAM dust model

The evolution of the dust field over the Mediterranean basin and its adjacent regions during the course of the campaign as predicted by the DREAM model can be found in the attached file that is listed below.

- Movie: Sm01.wmv

4 Vertical profile of the DREAM model and lidar observations

The campaign-mean vertical profile of the volume depolarization ratio and DREAM dust mass concentration is now provided in Fig. S4. On average, a prominent vertical dust profile is visible. Yet, the single data points at the sampling time/altitude show differences of several magnitudes, which is a similar result to our INP measurements.

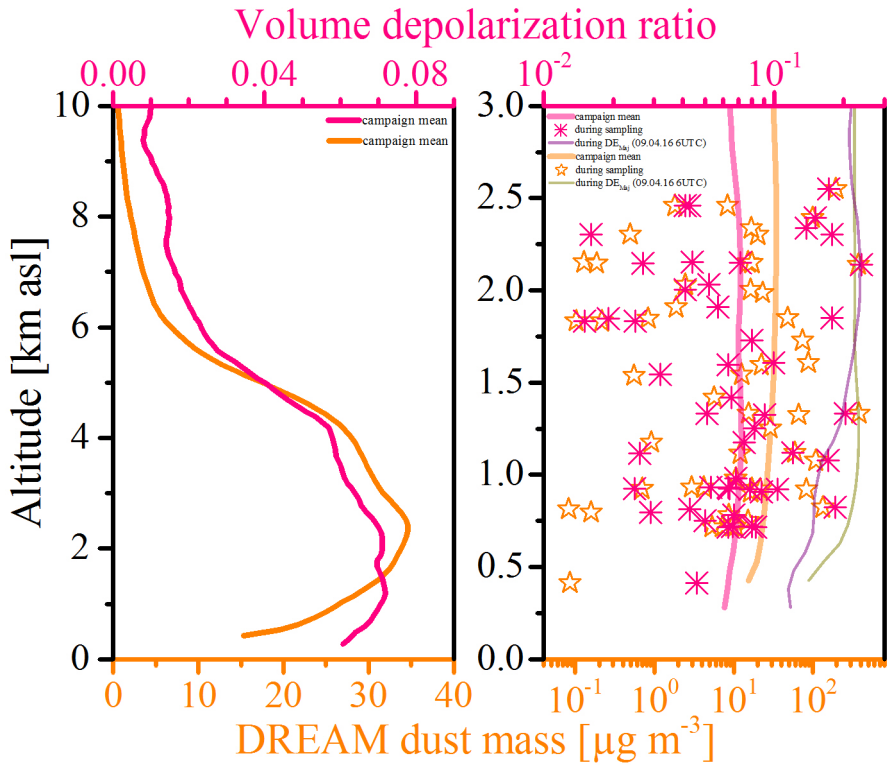

Figure 4. Left: Prominent vertical dust profile, when averaging over the whole campaign. Right: Large spread of single data points during INP sampling. Orange: DREAM dust mass concentration. Purple: Lidar volume depolarization ratio.

5 Comparison of active site densities

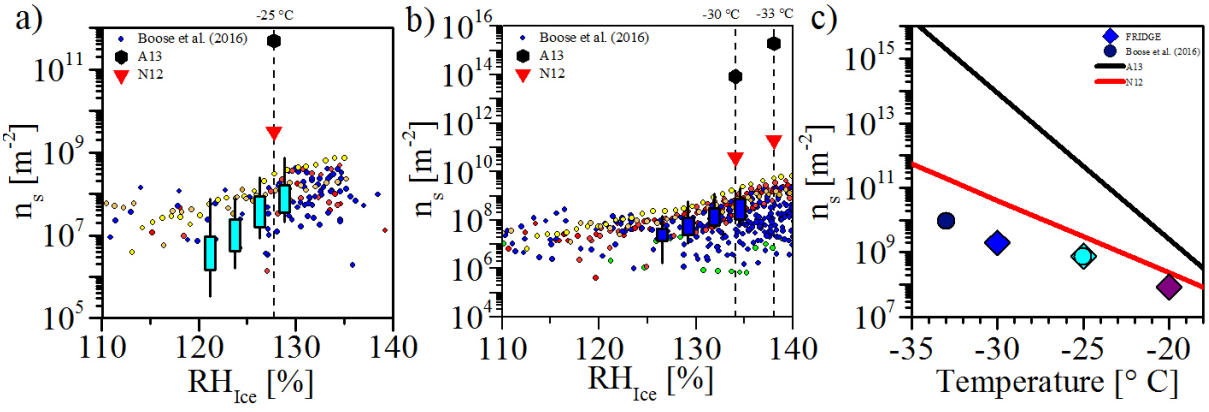

Figure 5. IN active site densities measured in the atmosphere and on mineral dust test aerosols. This study (boxes and diamonds); Boose et al. (2016) (circles); N12 (triangles and red line); A13 (hexagons and black line); dashed lines: water saturation at stated temperature.

References

Atkinson, J. D., Murray, B. J., Woodhouse, M. T., Whale, T. F., Baustian, K. J., Carslaw, K. S., Dobbie, S., O'Sullivan, D., and Malkin, T. L.: The importance of feldspar for ice nucleation by mineral dust in mixed-phase clouds, Nature, 498(7454), 355–8, doi:10.1038/nature12278, 2013.

Belyaev, S. P., and Levin, L. M.: Techniques for collection of representative aerosol samples, Journal of Aerosol Science, 5, doi:http://dx.doi.org/10.1016/0021-8502(74)90130-X, 1974.

Boose, Y., Sierau, B., García, M. I., Rodríguez, S., Alastuey, A., Linke, C., Schnaiter, M., Kupiszewski, P., Kanji, Z. A. and Lohmann, U.: Ice nucleating particles in the Saharan Air Layer, Atmospheric Chemistry and Physics, 16, 14, 9067–9087, doi:10.5194/acp-16-9067-2016, 2016.

Hagler, G. S. W., Yelverton, T. L. B., Vedantham, R., Hansen, A. D. A., and Turner, J. R.: Post-processing Method to Reduce Noise while Preserving High Time Resolution in Aethalometer Real-time Black Carbon Data, Aerosol and Air Quality Research, 11, 539–546, doi:10.4209/aaqr.2011.05.0055, 2011.

Hinds, W.C.: Aerosol Technology: Properties, Behaviors, and Measurement of Airborne Particles, Second Edition, John Wiley & Sons, Inc., New York, USA, 1999.

Niemand, M., Möhler, O., Vogel, B., Vogel, H., Hoose, C., Connolly, P., Klein, H., Bingemer, H., DeMott, P. and Skrotzki, J.: A particle-surface-area-based parameterization of immersion freezing on desert dust particles, J. Atmos. Sci., 69, 3077–3092, doi:10.1175/JAS-D-11-0249.1., 2012.